

## Communications to the Editor

### Adsorption of Polyethylene and Polypropylene by Zeolites: Inside or Outside?

Xingwu Wang,<sup>†</sup> Cristian C. Rusa,<sup>†</sup>  
Marcus A. Hunt,<sup>†</sup> Alan E. Tonelli,<sup>\*,†</sup>  
Tibor Macko,<sup>‡</sup> and Harald Pasch<sup>‡</sup>

Fiber & Polymer Science Program, North Carolina State University, Campus Box 8301, Raleigh, North Carolina 27695-8301, and German Institute for Polymers, Schlossgartenstr. 6, D-64289, Darmstadt, Germany

Received August 5, 2005

Revised Manuscript Received October 25, 2005

**Introduction.** Very recently, Macko et al.<sup>1–3</sup> reported for the first time that the highly hydrophobic polyolefins, polyethylene (PE) and isotactic polypropylene (PP), may be adsorbed from specific solutions onto certain zeolites. Once adsorbed, it was found, in both cases, to be very difficult to desorb the polyolefins from the zeolites. As a consequence, these authors concluded that both hydrophobic polyolefins likely penetrate and are at least partially included in the interiors of the narrow zeolite nanopores; i.e., in both cases the polyolefins are actually absorbed into the interiors of the zeolites. Buttersack et al.<sup>4</sup> and Matsui et al.<sup>5</sup> had previously observed poly(ethylene oxide), dextran, and poly(acrylic acid) and proteins and nucleic acids, respectively, to be adsorbed on zeolites. The former authors suggested penetration of zeolite pores during adsorption, while the latter assumed the biopolymers to be confined exclusively to the zeolite crystal surfaces. To date, no direct evidence has been provided concerning whether or not polymers adsorbed on zeolites actually penetrate their nanoporous crystals and remain included in the narrow zeolite channels. Here we describe attempts to determine whether PE and/or PP are adsorbed and reside on the

crystalline surfaces or are absorbed and penetrate and are included in the narrow nanoporous crystalline interiors when adsorbed on zeolites.

The pore structure<sup>6</sup> of the MF1-type zeolite SH-300, found<sup>1,2</sup> to strongly adsorb PE from its solutions in decalin, 1,3,5-trimethylbenzene, and 1,1,2,2-tetrachloroethane, is presented schematically in Figure 1. Pore/channel diameters range from ~5 to 6 Å. The Y zeolite CBV-780, found<sup>3</sup> to strongly adsorb PP, has a different and less confining pore structure<sup>7</sup> consisting of free cavities with diameters of 12 Å connected by 7.3 Å windows. This zeolite also contains larger mesopores (40–400 Å), but most are cavities not connected to the crystal surface. On the basis of previous modeling of PE<sup>8</sup> and PP<sup>9</sup> chain fragments isolated in narrow cylinders, we expect that PE and PP chains would and would not be able, respectively, to enter the SH-300 pores, while both polyolefins could penterate the pores in CBV-780. This is consistent with PP's inability to be adsorbed by the SH-300 zeolite.<sup>3</sup>

DSC and <sup>13</sup>C NMR observations of both polyolefins in their pure bulk and zeolite-adsorbed states are employed to probe the location of PE and PP chains adsorbed on zeolites. It is anticipated that PE and PP residing in the interior pore structures of zeolites would evidence an absence of thermal transitions (DSC-detected) that are apparent in their bulk samples, and their NMR spectra and the relaxation times derived from them would be distinct from those of the bulk polyolefins.

**Experimental Section. a. Materials.** The linear PE, with average molar mass  $M_w = 52$  kg/mol, isotactic PP, with  $M_w = 44.8$  kg/mol, and the zeolites (SH-300 and CBV-780) investigated here were described previously.<sup>1–3</sup> Decalin, diphenyl ether, and 1,2,4-trichlorobenzene (of synthesis quality) were obtained from Merck, Darmstadt, Germany.

An Ultra Stable faujasite zeolite CBV-780 with a Si/Al ratio of 40 was a product of Zeolyst Int., Valley Forge, PA. The CBV-780 crystals have an irregular spherical morphology. Zeolite SH-300 (Alsi-Penta Zeolithe GmbH,

<sup>†</sup> North Carolina State University.

<sup>‡</sup> German Institute for Polymers.

\* Corresponding author: e-mail alan\_tonelli@ncsu.edu.

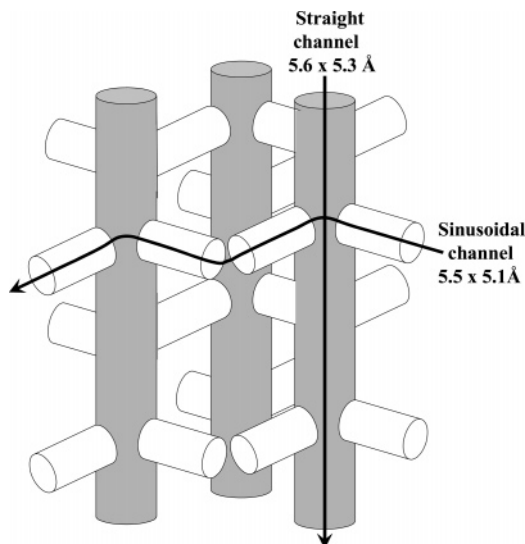


**Figure 1.** Schematic of the pore structure in zeolite SH-300.

Schwandorf, Germany) is a ZSM-5 material with a Si/Al ratio of 150. SH-300 has an average particle size of about 10  $\mu\text{m}$ . The pore structure of these zeolites is briefly described in the Introduction.<sup>1–3</sup> The adsorbents were dried before use by heating in an air atmosphere from room temperature to 450° C at a rate of 4.5 °C/min and were then held there for 4 h. Each zeolite was packed separately into a stainless steel column with a length of 150 mm and an internal diameter of 4.6 mm.

**b. High-Temperature Liquid Chromatography.** A high-temperature Waters 150C (Waters, Milford, MA) liquid chromatograph (LC) connected to an evaporative light scattering detector (PL-ELS 1000, Polymer Laboratories, Church Stretton, England) was used for the preparation of zeolites with the adsorbed polymers. The temperature of column, injector, and the mobile phase was set at 140° C. Hot solutions of PE in decalin or PP in diphenyl ether (200  $\mu\text{L}$  with concentration 1 mg polymer/mL) were injected many times into the column packed with either zeolite SH-300 or CBV-780. After the appearance of polymer peaks in the chromatograms, indicating no further pronounced adsorption of polyolefin, the column was purged with the mobile phase with the aim to remove any unadsorbed, unretained polymer. The column was then emptied, and the zeolite sorbent was washed with acetone to remove the previous mobile phase. Finally, the sorbent with the retained polymer was dried 7 days in a vacuum at 50° C. The amount of adsorbed polymer was calculated taking into account the volume of the polymer solution injected into the column and the weight of the dry zeolite sorbent in the column. The PE/SH-300 and PP/CBV-780 samples contained ~0.5 and 3.6 wt % adsorbed polyolefin, respectively.

**c. DSC.** Perkin-Elmer DSC-7 and TA Q1000 DSC instruments were employed to investigate the thermal characteristics of the bulk and zeolite-adsorbed samples of PE and PP. The sensitivities of our DSC instruments were tested by adding 1 wt % mixtures of PE powder with  $\text{Al}_2\text{O}_3$  powder of similar mesh size to the DSC pans. Melting endotherms for PE were readily detected in these control samples.

In addition, three control polyolefin/zeolite samples were prepared and observed by both DSC and  $^{13}\text{C}$  NMR. Enough zeolite SH-300 was added to a solution of PE in diphenyl ether (PE is not retained on SH-300 from

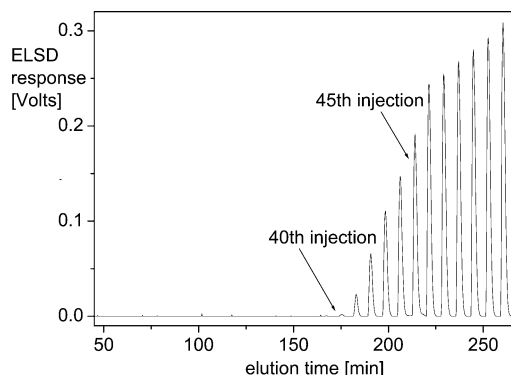


**Figure 2.** Chromatogram obtained after multiple injections of polyethylene (52 kg/mol) in decalin. Column packing: zeolite SH-300, 150 mm  $\times$  4.6 mm i.d. Mobile phase: decalin. Flow rate: 1 mL/min. Temperature: 140 °C.

diphenyl ether<sup>2,3</sup>) and to a solution of PP in 1,2,4-trichlorobenzene (PP is not retained on SH-300 from 1,2,4-trichlorobenzene and also PP is sterically precluded<sup>9</sup> from entering the pores in SH-300) to closely match the ~0.5 and 3.6 wt % polyolefin concentrations observed, respectively, to be adsorbed on these zeolites in the LC columns. The polyolefin solutions containing the suspended zeolites were then evaporated to dryness. The third control sample was similarly made using the CBV-780 zeolite and PP dissolved in 1,2,4-trichlorobenzene because PP was observed not to be adsorbed on CBV-780 from 1,2,4-trichlorobenzene in the LC experiments.<sup>1–3</sup> Approximately 5–10 mg samples of PE/SH-300 and PP/CBV-780 obtained by LC adsorption and the three control polyolefin/zeolite samples prepared by simple evaporation were employed and observed under nitrogen purge gas in two heating (10° C/min) and one cooling (200° C/min) scans between 25 and 200 °C.

**d.  $^{13}\text{C}$  NMR.** All solid-state NMR experiments were performed on a Bruker DSX-300 instrument operating at a field strength of 7.05 T, corresponding to a 300 MHz  $^1\text{H}$  Larmor frequency, using 7 mm zirconium oxide rotors.  $^{13}\text{C}$  cross-polarization/magic angle spinning/with high-power dipolar  $^1\text{H}$  decoupling (CP-MAS/DD) spectra, single-pulse MAS/DD spectra, and  $T_1(^{13}\text{C})$  measurements were performed with 4 kHz MAS and 3–3.5  $\mu\text{s}$   $\pi/2$  pulse widths. Radio-frequency field strengths for  $^1\text{H}$  decoupling (DD) were 70–73 kHz. The cross-polarization contact time was 1 ms, and the delay between two consecutive scans was 2–3 s, while single-pulse spectra were acquired with cycle delay times of 1 and 5 s.  $^{13}\text{C}$   $T_1$ 's were measured using the combination of cross-polarization and saturation-recovery pulse sequences.

**Results and Discussion.** Dilute decalin solutions of PE were injected many times into the column packed with zeolite SH-300 and flushed with pure decalin. The chromatogram in Figure 2 shows that polymer peaks appeared on the chromatogram after 40 injections of PE/decalin, when the column packing could no longer easily adsorb the injected polymer. The adsorption of PE continued, however, with ever decreasing adsorption of the injected polymer with increasing injection number. As a result, the heights of polymer peaks slowly increased (Figure 2). From independent measurements [Macko, T.; Brüll, R.; Pasch, H., manuscript in preparation] it is known that establishment of an adsorption equilibrium in this system requires at least 2 days. The chromatogram in Figure 2 indicates that PE is actually retained within the column packing. The amount of the adsorbed polymer was estimated from the number of

**Table 1.**  $^{13}\text{C}$  Spin–Lattice Relaxation Times,  $T_1(^{13}\text{C})$  in seconds, for Pure, Zeolite-Adsorbed, and Zeolite-Evaporated Control PE and PP Samples

polymer	$\text{CH}_3$	CH	$\text{CH}_2$
bulk PP	0.58	5.9	5.9
PP/zeolite	0.58, <sup>a</sup> 0.40, <sup>b</sup> 0.58 <sup>c</sup>	1.5, <sup>a</sup> 11, <sup>b</sup> 6.9 <sup>c</sup>	1.8, <sup>a</sup> 3.3, <sup>b</sup> 4.4 <sup>c</sup>
bulk PE			60
PE/SH-300			0.4, <sup>a</sup> 12 <sup>d</sup>

<sup>a</sup> PP/CBV-780 and PE/SH-300 LC adsorbed samples. <sup>b</sup> PP/CBV-780 evaporated control sample. <sup>c</sup> PP/SH-300 evaporated control sample. <sup>d</sup> PE/SH-300 evaporated control sample.

PE/decalin solution injections (for example, 45 injections, Figure 2). The same procedure was repeated with PP in the system diphenyl ether–zeolite/CBV-780. After removing the remaining mobile phase from the zeolites by filtration and vacuum-drying, the zeolite samples with the adsorbed polymers were analyzed by DSC and NMR.

Though containing similar amounts of PE and PP, the control samples of bulk PE mixed with  $\text{Al}_2\text{O}_3$  and the PE/SH-300, PP/SH-300, and PP/CBV-780 control samples obtained by simple evaporation showed melting endotherms in their heating DSC scans at the same temperatures ( $T_m$ ) as observed for pure bulk, semicrystalline PE and PP, while the samples (PE/SH-300 and PP/CBV-780) adsorbed on zeolites packed in the LC columns did not (DSC scans not shown). This indicates that, when adsorbed on SH-300 and CBV-780 zeolites, respectively, PE and PP chains are not able to aggregate and crystallize, consistent with their absorption and inclusion in the internal zeolite nanopores.

In Table 1, the spin–lattice relaxation times,  $T_1(^{13}\text{C})$ , observed for PE and PP carbon nuclei in bulk, evaporated, and zeolite-adsorbed samples are compared.  $T_1(^{13}\text{C})$ s for PE in bulk and zeolite-adsorbed samples are 60 and 0.4 s, respectively, a difference of  $\sim 2$  orders of magnitude. This dramatic increase in the megahertz librational motion has also been observed for PE guest chains isolated in the narrow channels ( $\sim 5$  Å) of its crystalline inclusion compound (IC) formed with the host perhydrotriphenylene (PHTP).<sup>10</sup>  $T_1(^{13}\text{C}) = 6.4$  s was observed for the PE chains included in the narrow PHTP channels, while the bulk sample had a  $T_1(^{13}\text{C}) = 320$  s. The similarity between both the dimensions of the nanopores in zeolite SH-300 and the channels in the PE-PHTP-IC and the reductions in the spin–lattice relaxation times observed for the guest PE chains also strongly point to absorption and inclusion of PE chains in the SH-300 zeolite nanochannels. Though a single short  $T_1 = 0.4$  s was observed for the adsorbed PE sample, distinct  $T_1$ s were observed for the crystalline and amorphous carbons in the bulk sample. Furthermore,  $T_1(^{13}\text{C}) = 12$  s, similar to bulk PE, is observed with the control sample, which was prepared by simple evaporation of solvent from the diphenyl ether/PE solution containing suspended SH-300 zeolite.

Though not as dramatic, the  $T_1(^{13}\text{C})$ s observed for PP adsorbed on the CBV-780 zeolite are also reduced (by a factor of 3–4) from those observed for bulk PP and PP evaporated on the surfaces of both CBV-780 and SH-300 zeolites, except for the rapidly rotating methyl carbons which evidence similar and much reduced  $T_1(^{13}\text{C})$ s for all samples. The general reduction in the  $T_1(^{13}\text{C})$ s observed for bulk crystalline PP compared with bulk crystalline PE samples is well-known<sup>11</sup> to be a result of the relaxation of  $^{13}\text{C}$  nuclear magnetization by the rapidly moving methyl protons. However, the

3–4-fold reduction in  $T_1(^{13}\text{C})$ s observed for the methylene and methine carbons in PP when adsorbed on zeolite-CBV-780 suggest segregated PP chains that have penetrated and reside in the internal zeolite nanochannels, where they have increased mobility compared to crystalline PP chains in both the bulk and evaporated control samples.

In Figure 3, the CP-MAS/DD and one-pulse MAS/DD  $^{13}\text{C}$  NMR spectra recorded for bulk PE, which are very similar to the spectra observed (Not shown) for PE simply evaporated on SH-300, are compared to the CP-MAS/DD spectrum of PE adsorbed on SH-300 in the LC column. All three spectra show two resonances at 35.2 and 33.3 ppm, which for bulk PE correspond respectively to methylene carbons in the crystalline and amorphous regions of the sample.<sup>12</sup> Because the mobility of PE chain segments in amorphous regions is much greater than in PE crystals, the single-pulse spectrum of bulk PE shows much greater intensity at 33.3 ppm, as does the CP-MAS/DD spectrum of PE adsorbed on SH-300 in the LC column, which is also very similar to its one-pulse MAS/DD spectrum (not shown). The PE chains adsorbed on SH-300 appear to be included in the zeolite nanochannels, where DSC observation indicated they are not able to crystallize, so the two distinct resonances observed there likely correspond to two populations of PE chain segments within different environments and/or with different conformations. The greater intensity observed for the high-field peak at 33.3 ppm may originate from PE chain segments residing in the larger cavities created at the intersections of straight and sinusoidal nanochannels in SH-300 (see Figure 1), while fewer PE chain segments resonating downfield at 35.2 ppm reside in the narrow zeolite channels far removed from their intersections. By analogy to bulk semicrystalline PE, this is consistent with all trans and magnetically shielding gauche bond<sup>12</sup> conformations respectively within the nanopores<sup>8</sup> and in the cavities created by their intersections in the SH-300 zeolite.

The CP-MAS/DD and one-pulse MAS/DD  $^{13}\text{C}$  NMR spectra of bulk PP are compared in parts a and b of Figure 4, respectively, and are very similar to the spectra recorded (not shown) for PP simply evaporated on the surfaces of the CBV-780 and SH-300 zeolites, which in the latter case cannot internally accommodate PP chains.<sup>3,9</sup> Note in the one-pulse spectrum only the methyl resonance at  $\sim 25$  ppm is prominent, while all three structurally distinct carbon nuclei resonate with significant intensities in the CP-MAS/DD spectrum, as a consequence of the 10-fold reduction in the  $T_1(^{13}\text{C})$  of the rapidly rotating methyl carbon compared with the methine and methylene carbon  $T_1(^{13}\text{C})$ s (see Table 1). On the other hand, the CP-MAS/DD (not shown) and one-pulse MAS/DD spectra (Figure 4c,d) observed for PP adsorbed on the CBV-780 zeolite are quite similar, consistent with both the much higher mobilities of their methine and methylene carbons when included in the zeolite pores and the absence of any rigid carbon nuclei, such as those observed for bulk semicrystalline PP and the evaporated control PP/zeolite samples (see Table 1), with PP adsorbed only on their surfaces. There is also a noticeable broadening and shifting of these resonances compared to pure crystalline PP, which adopts the 3<sub>1</sub>-helical ...tgtgtg... conformation, and this is consistent<sup>9,12,13</sup> with the presence of additional conformations available<sup>9</sup>



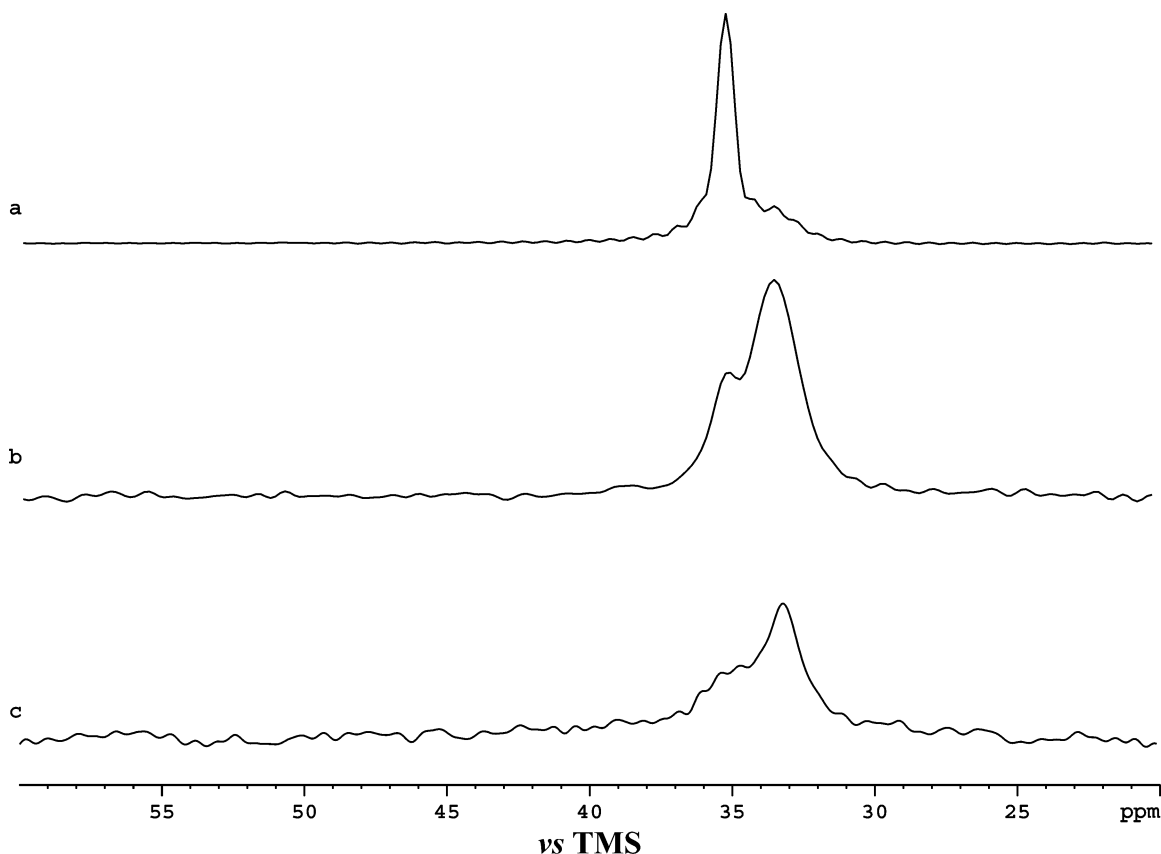


**Figure 3.** CP-MAS/DD (a) and one-pulse MAS/DD (b)  $^{13}\text{C}$  NMR spectra of bulk PE and (c) CP-MAS/DD  $^{13}\text{C}$  NMR spectrum of PE adsorbed from decalin at 140 °C onto zeolite SH-300 packed in an LC column.

to the PP chains absorbed in the nanopores of zeolite CBV-780.

**Summary and Conclusions.** DSC and  $^{13}\text{C}$  NMR observations of bulk, zeolite-evaporated, and zeolite-adsorbed PE and PP samples clearly point to significant inclusion of the adsorbed polyolefins in the internal nanopores of the respective zeolites, SH-300 and CBV-780, when packed in LC columns and repeatedly injected with PE/decalin and PP/diphenyl ether solutions maintained at 140° C. DSC scans show an absence of melting endotherms for both PE and PP when adsorbed by these zeolites packed in LC columns, which are, however, evident in their bulk and evaporated control samples. This supports the view that the adsorbed polymers have been separated by penetration and inclusion and are adsorbed in the narrow zeolite pores and therefore are unable to aggregate and crystallize, as would be possible if they were simply adsorbed on the zeolite surfaces.

Solid-state  $^{13}\text{C}$  NMR observations of bulk, evaporated control, and zeolite-adsorbed PE and PP samples may be summarized as follows: (1)  $T_1(^{13}\text{C})$  spin-lattice relaxation times observed for the PE and PP carbon nuclei when adsorbed on zeolites are dramatically to significantly reduced compared to those observed in their semicrystalline bulk and zeolite-evaporated samples. (2) The single-pulse MAS/DD spectra of bulk and evaporated (not shown) PE recorded without cross-polarization (CP) and the CP-MAS/DD spectrum of PE adsorbed on zeolite all show a major peak at 33.3 ppm (amorphous bulk) and a shoulder at 35.2 ppm (crystalline bulk), with intensities that are reversed from those observed in the CP-MAS/DD spectra of bulk and evaporated (not shown) PE. (3) The single-pulse MAS/DD and

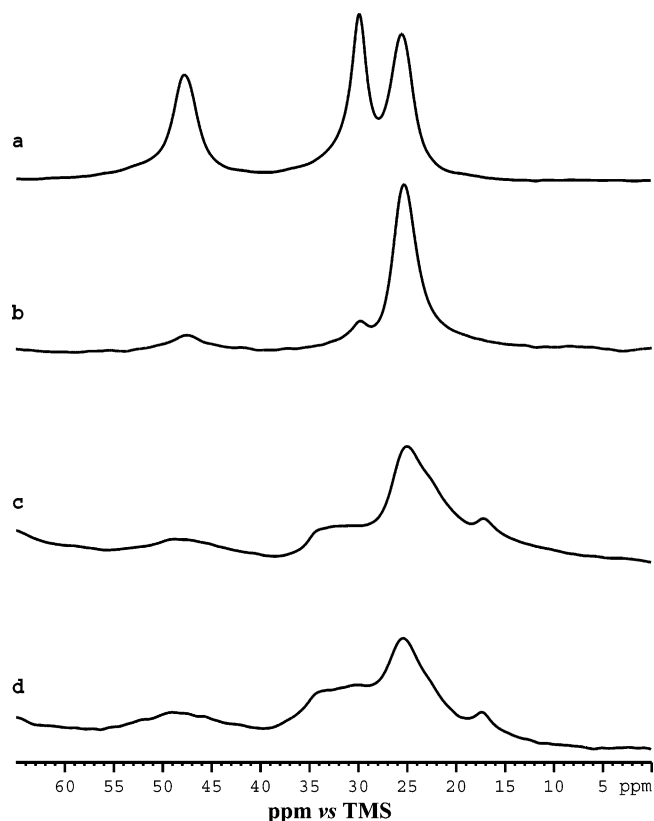


**Figure 4.**  $^{13}\text{C}$  NMR spectra of bulk and zeolite-adsorbed PP: (a) CPMAS/DD spectrum of bulk PP; (b, c, and d) one-pulse MAS/DD spectra of bulk (1 s cycle delay), zeolite-adsorbed (1 s cycle delay), and zeolite-adsorbed (5 s cycle delay) PP, respectively.

CP-MAS/DD spectra are remarkably different for both bulk and evaporated (not shown) PP, while those for PP adsorbed on zeolite are quite similar. (4) The methylene and methine carbon resonances in PP adsorbed on zeolite CBV-780 are significantly broader and shifted from the much narrower resonances observed in pure bulk and evaporated (not shown) PP.

We interpret these NMR observations as providing strong support for the inclusion of both polyolefins in the internal nanopores/channels of zeolites when they are adsorbed. In fact, in the case of PE adsorbed on zeolite SH-300 we suggest that most of the PE chain segments may occupy the larger internal cavities created by the intersection of zeolite nanochannels, with the remainder in the nanochannels far removed from their intersections (see Figure 1). In the larger zeolite cavities created by the intersecting nanopores, PE chains may be free to adopt magnetically shielding, gauche bond conformations, characteristic of those in amorphous regions of bulk PE, which may not be permitted in the more confining individual nanochannels, where only more extended conformations, such as the all-trans crystalline conformation of bulk PE, can fit. This is consistent with the large resonance peak observed at 33.3 ppm and the smaller shoulder at 35.2 ppm in the CP-MAS/DD spectrum of PE adsorbed on zeolite SH-300. The penetration of and inclusion in the narrow internal zeolite channels produces strong binding of both PE and PP chains that is manifested by the observed difficulty in desorbing both polyolefins.

These results are not totally unexpected on the basis of recent reports<sup>14–16</sup> of polymers absorbing into the narrow pores ( $\sim 5\text{--}10\text{ \AA}$ ) of channel structure  $\alpha$ - and  $\gamma$ -cyclodextrin crystals when they are suspended in polymer solutions. However, it is still not clear why such a migration of hydrophobic polymers dissolved in good

solvents occurs into the very narrow nanopores of host crystalline solids, such as the zeolites and cyclodextrins. It is supposed<sup>1–3</sup> that favorable absorption interactions are especially pronounced in the pores, which have dimensions comparable with the diameters of these extended polyolefin chains.

## References and Notes

- (1) Macko, T.; Pasch, H.; Denayer, J. F. *J. Chromatogr. A* **2003**, *1002*, 55.
- (2) Macko, T.; Denayer, J. F.; Pasch, H.; Baron, G. V. *J. Sep. Sci.* **2004**, *26*, 1569.
- (3) Macko, T.; Pasch, H.; Denayer, J. F. *J. Sep. Sci.* **2005**, *28*, 59.
- (4) Buttersack, C.; Rudolph, H.; Mahrholtz, J.; Buchholz, K. *Langmuir* **1996**, *12*, 3101.
- (5) Matsui, M.; Klyozumi, Y.; Yamamoto, T.; Mizushima, Y.; Mizukami, F.; Sakaguchi, K. *Chem.—Eur. J.* **2001**, *7*, 1555.
- (6) van Bekkum, H.; Flanigen, E. M.; Jansen, J. C. In *Studies in Surface Science and Catalysis*; Delmon, B., Yates, J. T., Eds.; Elsevier: Amsterdam, 1991; Vol. 58.
- (7) Janssen, A. H.; Koster, A. J.; de Jong, K. P. *Angew. Chem.* **2001**, *6*, 113.
- (8) Tonelli, A. E. *Macromolecules* **1990**, *23*, 3134.
- (9) Tonelli, A. E. *Macromolecules* **1991**, *24*, 3069.
- (10) Sozzani, P.; Bovey, F. A.; Schilling, F. C. *Macromolecules* **1991**, *24*, 6763.
- (11) Gomez, M. A.; Tanaka, H.; Tonelli, A. E. *Polymer* **1987**, *28*, 2227.
- (12) Tonelli, A. E. *NMR Spectroscopy and Polymer Microstructure: The Conformational Connection*; Wiley-Interscience: New York, 1989; Chapter 8.
- (13) Schilling, F. C.; Tonelli, A. E. *Macromolecules* **1980**, *13*, 270.
- (14) Rusa, M.; Wang, X.; Tonelli, A. E. *Macromolecules* **2004**, *37*, 6898.
- (15) Rusa, C. C.; Rusa, M.; Gomez, M. A.; Shin, I. D.; Fox, J. D.; Tonelli, A. E. *Macromolecules* **2004**, *37*, 7992.
- (16) Peet, J.; Rusa, C. C.; Hunt, M. A.; Tonelli, A. E.; Balik, C. M. *Macromolecules* **2005**, *38*, 537.

MA051748A